Journal of
Materials Chemistry C

Accepted Manuscript

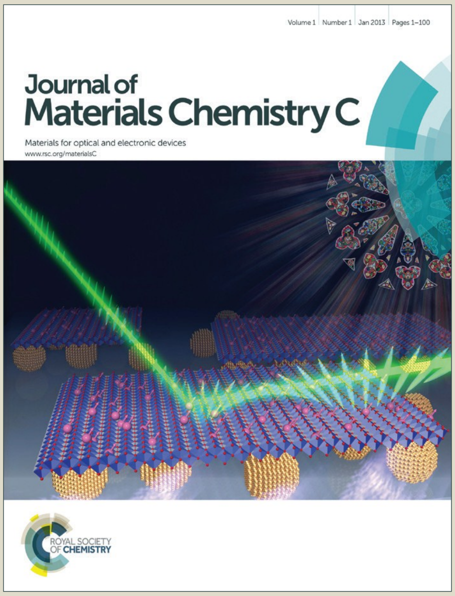

ROYAL SOCIETY
OF CHEMISTRY

www.rsc.org/materialsC

Cite this: DOI: 10.1039/c0xx00000x

www.rsc.org/xxxxxx

ARTICLE TYPE

Preparation of Bodipy-Ferrocene Dyads and Modulation of the Singlet/Triplet Excited State of Bodipy via Electron Transfer and Triplet Energy Transfer

Xueyan Wu,[a,b¶] Wenting Wu, [b¶] Xiaoneng Cui,[a] Jianzhang Zhao,[a*] and Mingbo Wu[b,*]

Received (in XXX, XXX) Xth XXXXXXXXX 20XX, Accepted Xth XXXXXXXXX 20XX
DOI: 10.1039/b000000x

Modulation of the singlet/triplet excited state of fluorophore is becoming more important for molecular valves, molecular memories, chemical or biological sensors and controllable PDT etc. Boron-dipyrromethene (Bodipy)-ferrocene (Fc) dyads were prepared for reversible electrochemical switching of the singlet excited state (fluorescence), as well as the triplet excited states of Bodipy. The photophysical properties of the dyads were studied with steady-state UV−vis absorption spectroscopy, fluorescence, electrochemical characterization, time-resolved fluorescence and nanosecond transient absorption spectroscopies. The fluorescence of the Bodipy moieties in the dyads was quenched significantly, due to the photo-induced electron transfer (PET). This conclusion was supported by electrochemical characterization and calculation of the Gibbs free energy changes of PET. We demonstrated that the fluorescence of the Bodipy moiety can be reversibly switched ON and OFF by electrochemical oxidation of the Fc moiety (Fc/Fc^+). Furthermore, we proved that the Fc moiety is efficient for quenching of the triplet excited state of Bodipy. Two quenching mechanisms, PET and triplet-triplet-energy transfer (TTET), are responsible for the *intramolecular* and *intermolecular* quenching of the triplet excited state of the diiodoBodipy unit.

Introduction

Modulation of the singlet/triplet excited state of chromophores is important for photocatalysis,[1−3] molecular valves, [4,5] molecular memories,[6] chemical or biological sensors[7] and controllable photodynamic therapy (PDT),[8−13] etc. On the other hand, modulation of singlet/triplet excited state of chromophores will present additional dimension to the application of fluorophore in various areas. For example, modulation of the excited state of chromophores with an external-stimuli responsive unit in the multi-chromophore molecules will lead to functional compounds, such as fluorescent molecular probes,[14−17] and activatable PDT reagents.[4,18−20] Concerning these aspects, ferrocene (Fc) is in particular interest due to its redox centre displays an outstanding reversible redox behaviour and its electron-donating ability can be modulated by electrochemical oxidation reversibly. Fc has been extensively used for studying the electron transfer in molecular dyads and triads, as well as in controlling the fluorescence via PET.[21,22] For example, previously it was shown that Fc is a strong electron donor in Fc-Bodipy-C_{60} triad, in the PET process.[23] Fc-Bodipy dyad was used as a viscosity probe, the quenching mechanism was attributed to the free rotor effect.[24] However, the quenching effect of Fc on the triplet excited state of organic chromophores, especially those show strong absorption of visible light and long-living triplet state, was rarely studied.[21,22]

Previously the quenching of triplet excited state of organic chromophores by Fc via intermolecular triplet energy transfer (EnT) or electron transfer (ET) were studied.[25] But the triplet state energy donors studied were limited to the polycyclic aromatic hydrocarbons, such as anthracene and naphthalene, etc.[25] Photophysics of the Fc-perylenediimide (PDI) dyad and triads were studied, PET with Fc as electron donor was confirmed with femtosecond transient absorption spectra, and it was found that the triplet state of PDI moiety was formed by charge recombination (CR).[26] The photo-induced intramolecular ET was studied with C_{60}-Fc dyad.[27] Ultrafast photo-induced charge separation and electron shift was reported with C_{60}-NDI-Fc triad (NDI = naphthalenediimide).[28] The photoinduced electron transfer in Fc-azaBodipy dyad and triad was studied, but the azaBodipy part in the dyad and triad is unable to produce triplet excited state efficiently.[29] To the best of our knowledge, the effect of the Fc moiety on the triplet excited state of the visible light-harvesting organic chromophores was not studied.[21]

Herein we prepared Fc-Bodipy and Fc-diiodoBodipy dyads with different linkers between the two chromophores in the dyads (**B−1**, **B−2** and **B−3**. Scheme 1), with the aim to study the modulation effect of Fc on the singlet excited state and triplet excited state of Bodipy. To the best of our knowledge, it is the first time that controlling of the triplet excited state of Bodipy by Fc was studied. Furthermore, we switched the fluorescence of Bodipy chromophore via reversible redox manipulation of the Fc unit in the dyads. The photophysical properties of the Fc-Bodipy and Fc-diiodobodipy dyads were studied with steady-state UV−vis absorption spectra, fluorescence spectra, spectroelectrochemistry and nanosecond transient absorption spectroscopy. The intermolecular electron and energy transfer processes were studied. We found that the fluorescence of the Bodipy can be reversibly switched by electrochemical oxidation and reduction of the Fc moiety (via spectroelectrochemical method), and the triplet excited state of 2,6-diiodoBodipy moiety can be quenched by both the electron transfer and triplet-triplet energy transfer (TTET) processes.

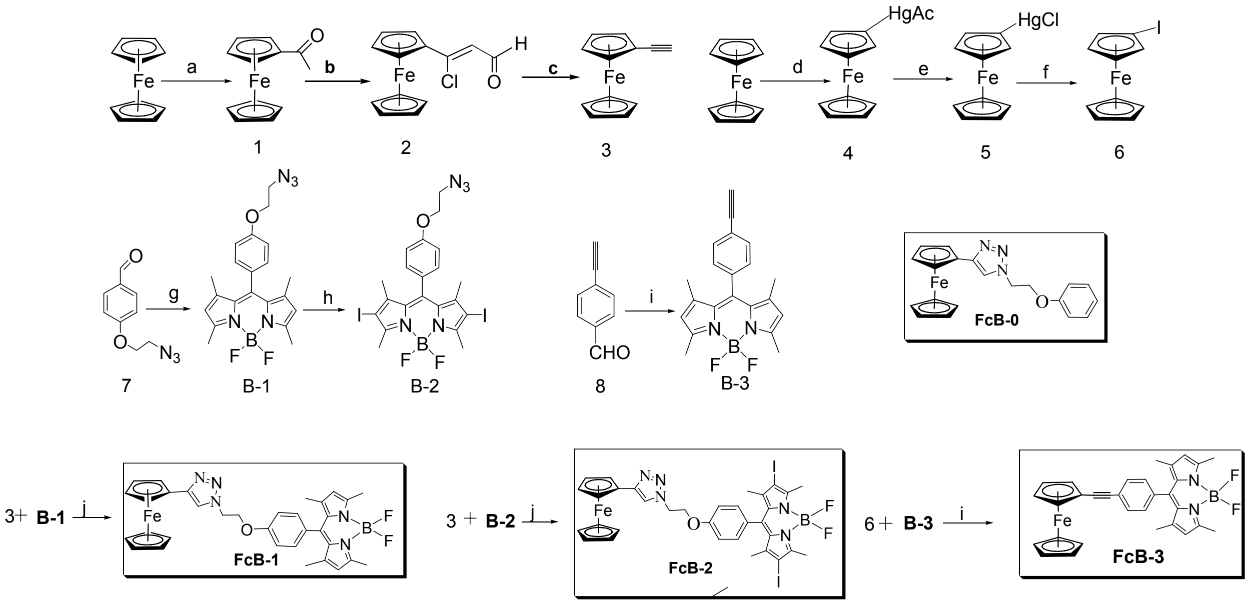

Scheme 1. (a) Acetyl chloride and $AlCl_3$, DCM, 25 °C, Ar, 30-60 min; yield 75.3%; (b) $POCl_3$/DMF, 0 °C, Ar, 1.5 h. NaOAc, 25°C, Ar, 1 h; yield 76.3%; (c) 1,4-dioxane, NaOH, reflux,0.5 h; yield 90.7%; (d) HgOAc, MeOH / benzene, 25 °C, Ar,12 h; (e) LiCl, EtOH-H_2O mixture, 25 °C, Ar, 1 h; yield 60.8 %; (f) NIS, dry DCM, 0 °C, Ar, 12 h; $NaHSO_3$; yield 74.7%; (g) Ar, DCM, TFA, DDQ, Et_3N and $BF_3{\cdot}Et_2O$; (h) NIS, dry DCM, 25 °C, Ar, 12 h; (i) $Pd(PPh_3)_2Cl_2$, PPh_3, CuI, THF, NEt_3, Ar, 90 °C, 8 h; (j) sodium ascorbate, $CuSO_4$, 25 °C, Ar, 60 h.

Experimental Section

Analytical Measurements.

All the chemicals are analytically pure and were used as received. Solvents were dried and distilled prior to use. ^1H and ^{13}C NMR spectra were recorded with Bruker 400/500 MHz spectrophotometer ($CDCl_3$ as solvent, TMS as standard for which δ = 0.00 ppm). High resolution mass spectra (HRMS) were determined with MALDI-HRMS, ESI-Q-TOF MS spectrometer.

Synthesis of complex B−1.

Under Ar atmosphere, a mixture of **7** (1.91 g, 10 mmol) and 2,4-dimethylpyrrole (1.88 g, 20 mmol) in dry CH_2Cl_2 (250 mL) was stirred at rt. Then TFA (0.1 mL) was added into the mixture by syringe and the mixture was stirred at RT overnight. DDQ (1.13 g, 5 mmol) was dissolved in dry CH_2Cl_2 (30 mL) and the solution was poured into the mixture in one portion, then the mixture was stirred at RT for 7 h. Triethylamine (10 mL) was added dropwise into the mixture with cooling by ice bath. The reaction mixture was stirred for another 0.5 h. Then $BF_3{\cdot}Et_2O$ (10 mL) was added dropwise into the mixture. The reaction mixture was stirred overnight. The solution was concentrated under reduced pressure and water (200 mL) was added. The mixture was stirred for 24 h. Then the solution was extracted with CH_2Cl_2 (3 × 100 mL) and the organic layer was dried over anhydrous Na_2SO_4. The solvent was evaporated under reduced pressure. The crude product was purified by column chromatography (silica gel, CH_2Cl_2/ petroleum ether = 1:1, v/v) to give **B−1** as red solid. Yield: 300 mg (7.5 %). M.p. 146.5–148.4 °C. ^1H NMR (400 MHz, $CDCl_3$) δ 7.21 (d, J = 12.0 Hz ,2 H), 7.05 (d, J = 12.0 Hz, 2H), 5.98 (s, 2H), 4.21 (t, J = 4.0 Hz, 2H), 3.67 (t, J = 4.0 Hz, 2H), 2.55 (s, 6H), 1.43 (s, 6H). MALDI-HRMS: m/z calcd for $[C_{21}H_{22}N_5OBF_2]^+$ 409.1885; found: m/z = 409.1859.

Synthesis of complex B−2.

To a solution of **B−1** (200 mg, 0.49 mmol) in anhydrous CH_2Cl_2 (25 mL) was added *N*-iodosuccinimide (NIS, 558 mg, 2.48 mmol). The mixture was stirred at 30 °C overnight. The reaction mixture was concentrated under vacuum, and the residue was purified by column chromatography (silica gel. petroleum ether /CH_2Cl_2=2:1, v/v). The red band was collected, and the solvent was removed under reduced pressure to give the product as red solid. Yield: 280.0 mg (90.4 %). M.p. 168.7–170.2 °C. ^1H NMR (400 MHz, $CDCl_3$) δ 7.17 (d, J = 8.0 Hz, 2H), 7.07 (d, J = 8.0 Hz, 2H), 4.24 (t, J = 4.0 Hz, 2H), 3.69 (t, J = 4.0 Hz, 2H), 2.65 (s, 6H), 1.45 (s, 6H). MALDI-HRMS: m/z calcd for $[C_{21}H_{20}N_5OBF_2I_2]^+$ m/z = 660.9804; found: m/z = 660.9817.

Synthesis of complex B–3.

Under Ar atmosphere, to a solution of 4-ethynylbenzaldehyde **8** (400.0 mg, 3.0 mmol) and 2,4-dimethylpyrrole (672 mg, 7.0 mmol) in CH_2Cl_2 (250 mL) was added trifluoroacetic acid (2.3 mL, 0.034 mmol). The mixture was stirred at RT for 1 h then *p*-chloranil (756.0 mg, 3.0 mmol) was added. The mixture was stirred at RT for another 1 h. NEt_3 (5.26 g, 52.0 mmol, 7.2 mL) was added, and the mixture was stirred for 10 min. Then $BF_3 \cdot OEt_2$ (8.02 g, 55.3mmol) was added via syringe and the mixture was stirred for another 10 min. The reaction mixture was washed with water (4 × 60 mL) and dried with anhydrous Na_2SO_4. The solvent was removed under vacuum and the residue was purified by chromatography (silica gel, petroleum ether /CH_2Cl_2=1:1, v/v) to give compound **B–3** as an orange solid. Yield: 320 mg (28.9 %). M.p. 243.1–245.4 °C. ^{1}H NMR (400 MHz, $CDCl_3$): δ 7.62 (d, *J* = 8.0 Hz, 2H), 7.26 (d, *J* = 8.0 Hz, 2H), 5.99 (s, 2H), 3.18 (s, 1 H), 2.56 (s, 6H), 1.40 ppm (s, 6H). TOF HRMS EI$^+$: calcd ([$C_{21}H_{19}BN_2F_2$]) *m/z* = 348.1609; found, *m/z* = 348.1617.

Synthesis of complex FcB–0

Under Ar atmosphere, ethylnylferrocene (21.0 mg, 0.1 mmol) and **3** (20 mg, 0.1 mmol) were dissolved in mixed solvent $CHCl_3/MeOH/H_2O$ (8 mL, 6:1:1, v/v). Then $CuSO_4 \cdot 5H_2O$ (7.5 mg) and sodium ascorbate (11.5 mg) was added. The resulting mixture was stirred at 25 °C for 16 h. Then the reaction mixture was washed with water and extracted with CH_2Cl_2 (3×50 mL). The organic layer was dried over anhydrous Na_2SO_4 and evaporated under reduced pressure. The crude product was purified by column chromatography (silica gel, CH_2Cl_2) to give a red solid. 18.0 mg, yield: 43.9 %. M.p. 132.5–134.8 °C. ^{1}H NMR (400 MHz, $CDCl_3$) δ 7.66 (s, 1H), 7.32 (t, *J* = 16 Hz, 2H), 7.01 (t, *J* = 16 Hz, 1H), 6.91 (d, *J* = 8.0 Hz , 2H), 4.78 (t, *J* = 8.0 Hz, 2H), 4.72 (s, 2H), 4.40 (t, *J* = 8.0 Hz, 2H), 4.30 (s, 2H), 4.07 (s, 5H). TOF HRMS EI$^+$: calcd ([$C_{20}H_{19}N_3OFe$]) *m/z* = 373.0878, found, *m/z* = 373.0871.

Synthesis of complex FcB–1

Complex **FcB–1** was prepared by a similar procedure to that for complex **FcB–0**, with ethylnylferrocene (21.0 mg, 0.1 mmol) and **B–1** (44 mg, 0.1 mmol) as the starting material, instead of **3**. Complex **FcB–1** was obtained as a red solid 48.0 mg, yield: 77.4 %. M.p. 211.8–212.6 °C. ^{1}H NMR (400 MHz, $CDCl_3$) δ 7.57(s, 1H), 7.17 (d, *J* = 8.0 Hz, 2H), 7.00 (d, *J* = 8.0 Hz, 2H), 5.96 (s, 2H), 4.98 (s, 2H), 4.78 (s, 2H), 4.54 (s, 2H), 4.42 (s, 2H), 4.25 (s, 5H), 2.54 (s, 6H), 1.39 (s, 6H). ^{13}C NMR (100 MHz, $CDCl_3$) δ = 158.45, 155.47, 154.20, 147.06, 143.07, 141.09, 131.73, 129.54, 128.22, 121.20, 115.12, 111.23, 99.96, 91.17, 66.75, 57.93, 50.33, 14.69, 14.59. MALDI-HRMS: *m/z* calcd for [$C_{33}H_{32}N_5OBF_2Fe$]$^+$ *m/z* = 619.2017; found: *m/z* = 619.2028.

Synthesis of complex FcB–2

Complex **FcB–2** was prepared by a similar procedure to that for complex **FcB–1**, with ethylnylferrocene (21.0 mg, 0.1 mmol) and **B–2** (66 mg, 0.1 mmol) as the starting material, instead of **B–1**. Complex **FcB–1** was obtained as a deep red solid 65.3 mg, yield: 73.6 %. M.p. 235.8–237.6 °C. ^{1}H NMR (400 MHz, $CDCl_3$) δ 7.63 (s, 1H), 7.15 (d, *J* = 8.0 Hz, 2H), 7.02 (d, *J* = 8.0 Hz, 2H), 4.81 (t, *J* = 8.0 Hz, 4H), 4.46 (t, *J* = 8.0 Hz, 2H), 4.39 (s, 2H), 4.13 (s, 5H),2.63 (s, 6H), 1.39 (s, 6H). ^{13}CNMR (100 MHz, $CDCl_3$) δ = 158.78, 156.86, 145.47, 141.06, 131.68, 129.72, 127.96, 116.65, 106.58, 96.08, 85.66, 68.84, 52.91, 29.50, 18.02, 16.09. MALDI-HRMS: *m/z* calcd for [$C_{33}H_{30}N_5OBF_2FeI_2$]$^+$ *m/z* = 870.9950; found: *m/z* = 870.9945.

Synthesis of complex FcB–3

Iodoferrocene (62.4 mg, 0.2 mmol) was added to a deaerated solution of **B–3** (69.6 mg, 0.2 mmol) in THF (15 mL) and triethylamine (5 mL) (deoxygenated by Ar for 15 min). After the mixture was stirred for 10 min, [$PdCl_2(PPh_3)_2$] (14.0 mg, 0.02 mmol) and CuI (3.8 mg, 0.02 mmol) were added into the solution, then the mixture was refluxed for 8 h. After being cooled to RT, the reaction mixture was poured into water, and the aqueous phase was extracted with CH_2Cl_2 (50 mL). The combined organic extracts were washed with water (50 mL) and then brine (50 mL) and dried over anhydrous Na_2SO_4. The mixture was filtered, concentrated under reduced pressure, and purified by chromatography (silica gel; CH_2Cl_2 / petroleum ether = 1/ 4, v/v) to give a deep-red solid. Yield: 30.4 mg (28%). ^{1}H NMR (400 Mz, $CDCl_3$) δ 7.62 (d, *J* = 8.0 Hz, 2H), 7.24 (d, *J* = 4.0 Hz, 2H), 5.99 (s, 2H), 4.53 (t, *J* = 4.0 Hz, 2H), 4.28 (s, 7H), 2.56 (s, 6H), 1.44 (s, 6H). MALDI-HRMS: calcd ([$C_{31}H_{27}BF_2$ FeN_2]$^+$) *m/z* = 532.1585, found, *m/z* = 532.1611.

Nanosecond Time-Resolved Transient Difference Absorption Spectroscopy

The nanosecond time-resolved transient absorption spectra were recorded on LP920 laser flash photolysis spectrometer (Edinburgh Instruments, UK). The samples were excited with a nanosecond pulsed laser (Opotech, wavelength tunable in the range of 410 – 2400 nm), and the transient signals were recorded on a Tektronix TDS 3012B oscilloscope. All samples in flash photolysis experiments were deaerated with nitrogen for ca. 15 min before measurement.

Spectroelectrochemical Studies

Spectroelectrochemical fluorescence measurements were performed with a spectra-electrochemical quartz cell (path-length of 1.0 mm) using a three-electrode system: light transparent platinum gauze (100 mesh, 7.0 × 5.0 mm) as a working electrode, a platinum wire counter electrode, and an Ag wire reference electrode. Potentials were applied with a CHI610d electrochemical workstation. The electrochemical reaction was monitored with a RF5301PC spectrofluorometer (Shimadzu, Japan) spectrofluorometer. All electrochemical measurements were carried out under nitrogen atmosphere.

Results and discussion

Design and Synthesis of the Fc-Bodipy Dyads

Due to the intense visible light absorption, high fluorescence quantum yields and feasible derivatization,[16,30–33] boron dipyrromethene (BODIPY) was selected as the organic chromophore. Ferrocene, the strong electron donor in PET process, was selected to tune the singlet and triplet excited state of organic chromophores. The linker between Fc and Bodipy could greatly influence the electron and energy transfer, so various linkers, e.g. acetylide and Click 1,2,3-triazole, were firstly used in dyads **FcB–1** and **FcB–3** to tune the quenching effect of Fc on the singlet excited state of organic chromophores (Scheme 1), which benefits the subsequent study of the quenching effect on triplet excited states. Compared with acetylide connection, Click 1,2,3-triazole shows moderate electron transfer rate (vide infra), which benefits the definite study about the quenching effect of electron and energy transfer on triplet excited state of organic chromophores respectively. Thus **FcB–2** was devised, wherein Click 1,2,3-triazole connects the Fc and the 2,6-diiodoBodipy parts together. (Scheme 1). Compounds **B–1**, **B–2** and **B–3** were prepared as references for the study of the photophysical properties of the dyads (Scheme 1). All the compounds were obtained with moderate to satisfactory yields. The molecular structures were fully verified with ^{1}H NMR, ^{13}C NMR and HRMS spectra. Compounds **1**, **2**, **3**, **5**, **6**, **7**, **8** were synthesized according to previously reported methods (see ESI † for synthesis and molecular structural characterization data).

Steady-state Electronic Spectroscopy (UV–vis Absorption and Emission Spectra)

The UV–vis absorption spectra of the compounds were studied (Fig. 1). Fc as electron donor moieties in Fc-Bodipy dyads does not show any significant absorption in the visible region, while Bodipy shows intense absorption in the visible region. For **FcB–1,** it shows similar absorption as compared with that of the reference compound **B–1**, especially in the visible spectral region (Fig. 1a). This result indicates that there is no significant electronic interaction between the Fc and the Bodipy moieties in **FcB–1** at the ground state. Similar results were observed for **FcB–2** and **FcB–3** (Fig. 1b and 1c). The UV–Vis absorption spectra of compounds do not show significant solvent dependency (see ESI †, Fig. S31–S32), further indicating that the ground state were not affected by the solvent polarity or hydrogen bonding. Actually, these dyads show the supramolecular feature of the dyads concerning the photophysical properties (i.e. a light harvesters show one major absorption bands corresponding to one chromophore).[33–36]

The fluorescence of the compounds was also studied (Fig. 1). In order to compare the fluorescence of the dyads with that of the reference compounds, optically matched solutions (the solutions in comparison show the same absorbance at the excitation wavelength. Thus the concentration of the solution varied slightly) were used (Fig. 1). For **FcB–1**, the fluorescence band is centered at 516 nm, similar to the fluorescence emission of the reference compound. However, the fluorescence intensity of **FcB–1** is much weaker than that of **B–1** (Fig. 1d). Similar quenching effect on the fluorescence of the reference compounds were observed for **B–2**/**FcB–2** and **B–3**/**FcB–3** (Fig. 1e and 1f**)**, and the quenching effect in **FcB–2** is weaker than that in **FcB–1** and **FcB–3**.

Based on the absorption spectra and the quenching effects, the PET mechanism is proposed to be responsible for the fluorescence quenching in the dyads.[37] At the ground state, there is no significant electronic interaction between the Fc and the Bodipy moieties in the dyads (Fig. 1a, 1b, 1c). Conversely, emission quenching effects of **FcB–1** ~ **FcB–3** happen upon irradiation, indicating that PET process occurs at the excited state from the Fc moiety (strong electron donor) to the singlet excited state of Bodipy (electron acceptor fluorophore). The PET mechanism was also confirmed by the calculation of the Gibbs free energy changes ($\Delta G°$, vide infra), and these results were agreed with the experimental data reported before.[26,28,29] To the best of our knowledge, this is the first study of the fluorescence quenching of Bodipy by Fc based on the PET mechanism. It should be pointed out that Fluorescence resonance energy transfer (FRET) is unlikely the quenching mechanism, because Fc does not show strong absorption in the emission region of the Bodipy moiety (note large molar extinction coefficient of the energy acceptor is mandatory for efficient FRET).[38]

The solvent polarity-dependence of the fluorescence of the dyads were studied and compared with the organic references (Fig. 2). The luminescence spectra of optically matched solutions of **FcB–1** in different solvents are presented in Fig. 2a.

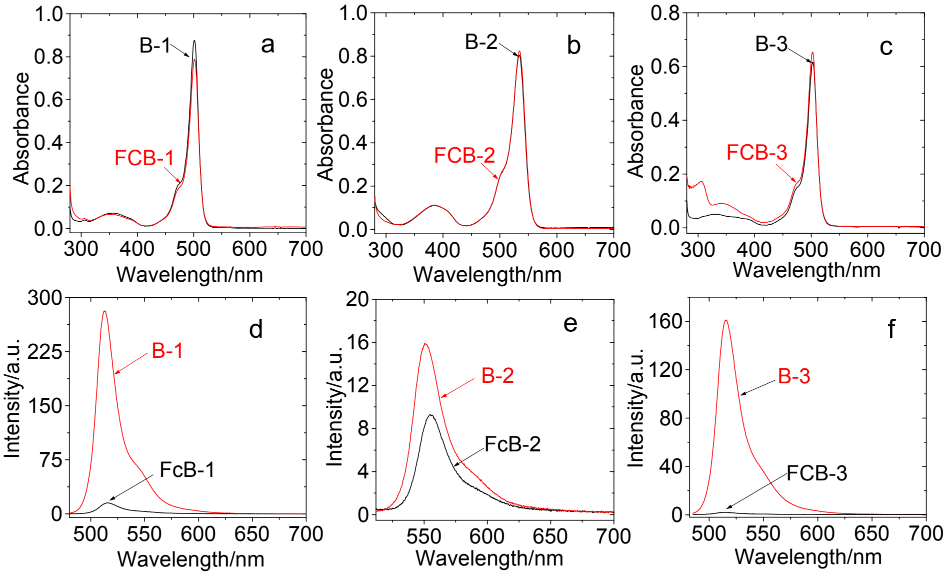

Fig. 1 UV–vis absorption of (a) **B–1** and **FcB–1**. (b) **B–2** and **FcB–2**. (c) **B–3** and **FcB–3**. The fluorescence emission spectra of (d) **B–1**, **FcB–1** (λ_{ex} = 475 nm, A = 0.194). (e) **B–2** and **FcB–2** (λ_{ex} = 508 nm, A = 0.291) and (f) **B–3**, **FcB–3** (λ_{ex} = 482 nm, A = 0.313). Optically matched solutions were used. c =1.0 × 10^{-5} M in DCM, 20 °C.

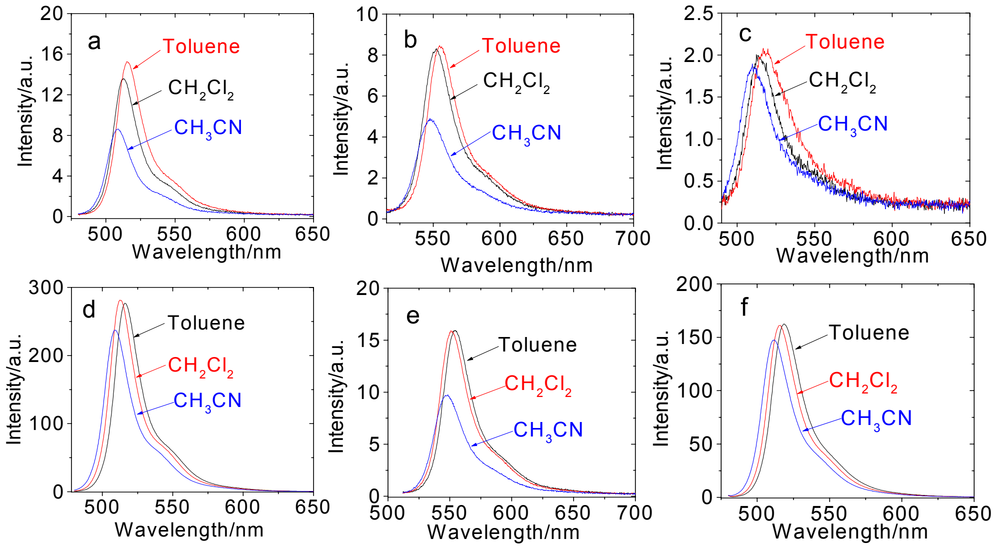

Fig. 2 The emission spectra of (a) **FcB–1** (λ_{ex} = 474 nm A = 0.171), (b) **FcB–2** (λ_{ex} = 508 nm, A = 0.307) , (c) **FcB–3** (λ_{ex} = 482 nm, A = 0.149) (d) **B–1** (λ_{ex} = 475 nm, A = 0.209), (e) **B–2** (λ_{ex} = 508 nm, A = 0.281) and (f) **B–3** (λ_{ex} = 478 nm, A = 0.194) in toluene, CH_2Cl_2 and CH_3CN. Optically matched solutions were used c = ca. 1.0 × 10^{-5} M (the concentrations were varied slightly to attain optically matched solutions). 20 °C.

The fluorescence is weaker in acetonitrile than that in less polar solvents, such as toluene. There is a slight blue-shift of the band maxima in passing from toluene to dichloromethane, then to acetonitrile. For the reference compound **B–1** (Fig. 2d), however, no such clear dependence was observed. This result indicated the PET process happened in **FcB–1**. For **FcB–2**, the fluorescence intensity in dichloromethane is essentially identical to that in toluene, while it decreases obviously in acetonitrile. Similar solvent polarity-dependent fluorescence emission was observed for **B–2**. No strong polarity-dependent fluorescence was observed for **FcB–3** (Fig. 2c), as well as for the reference compound **B–3** (Fig. 2f).[24]

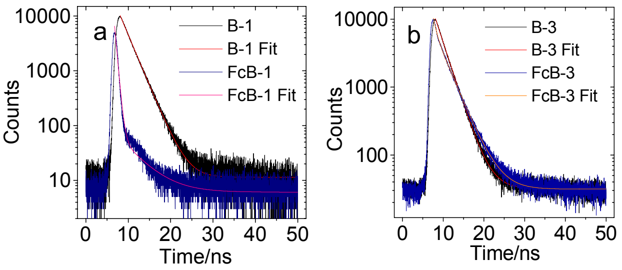

Fig. 3 Decay profiles of fluorescence lifetime measurement of (a) **FcB–1** and **B–1** ;(b) **FcB–3** and **B–3** (c = 1.0 × 10^{-5} M) in DCM. 20 °C.

The fluorescence decay of compounds **FcB–1**, **FcB–3** and the reference Bodipy compounds **B–1** and **B–3** was recorded at 512 nm upon excitation with 445 nm picosecond laser (Table 1). For **B–1**, a single exponential decay trace was observed (Fig. 3a), which gives a fluorescence lifetime of 3.72 ns (Table 1). For the dyad **FcB–1**, however, a clear biexponential decay of the emission was observed, which contains a short fluorescence lifetime (τ_1 = 0.42 ns, 85.2%) and a longer lifetime component τ_2 = 4.29 ns, 14.8%). The shorter lifetime can be attributed to the charge separation process (with which the fluorescence of the Bodipy chromophore was quenched), whereas the longer lifetime component is close to the intrinsic fluorescence lifetime of Bodipy (3.72 ns).

Previously a biexponential decay trace was observed for the Fc–PDI dyad, for which the quenching of the fluorescence of PDI was attributed to PET.[39] Similar results were observed for **B–3** (Fig. 3b). For **B–3**, the decay obeyed single exponential function giving a single fluorescence lifetime (τ= 2.42 ns). On the other hand, the decay of triad **FcB–3** consisted of a fast decay component (τ_1 = 0.64 ns, 19%) and slow component (τ_2 = 2.78 ns, 81%). From the shorter lifetime compared with **B–3**, an appreciable increase in the decay rate of triad **FcB–3** was observed. The shorter τ_1 value (0.64 ns) of triad **FcB–3** can be attributed predominantly to charge separation between the Fc and Bodipy moieties, while the longer τ_2 value (2.78 ns) is similar to the intrinsic fluorescence lifetime of the **B–3** chromophore (2.42 ns).

Based on the fluorescence quenching in dyads and the intrinsic fluorescence lifetimes of the Bodipy parts in the dyads (from the reference compounds **B-1**, **B-2** and **B-3**), the electron transfer rate constants in the dyads were calculated with Eq.1.[40]

$$k_{\mathrm{ET}} = \frac{1}{\tau_{\mathrm{Dyads}}} - \frac{1}{\tau_{\mathrm{Ref}}} \qquad \text{(Eq. 1)}$$

τ_{Ref} is the lifetime of the reference compounds (**B–1** or **B–3**) and τ_{Dyads} is the lifetime of the Dyads (**FcB–1** or **FcB–3**). The data were compiled in Table 1.

Electron transfer rate constant of the PET process in compound **FcB–3** is (1.15 ± 0.06) × 10^{9} s^{-1}, which is much smaller than that in **FcB–1** (2.11 ± 0.11) × 10^{9} s^{-1}). This result indicates that the linker between the chromophores is crucial for the electron transfer. We also used a Click reaction to connect the Fc and the 2,6-diiodoBodipy parts together (a moderate linker) to study the quenching effect of Fc on triplet excited state of organic chromophores (**FcB–2**) from electron and energy transfer respectively. The electron transfer rate constant of **FcB-2** is 1.39 ± 0.07) × 10^9 s^{-1}. The electron transfer rate constants of the dyads are in agreement with the fluorescence quanching studies (Fig. 2).

Electrochemical Study (Cyclic Voltammetry) and Gibbs free energy changes of PET

The redox properties of the compounds were studied with cyclic voltammetry (Fig. 4). For **B–1**, a reversible oxidation wave at $E_{1/2}$ = +0.95 V was observed. A reversible reduction wave at $E_{1/2}$ = −1.53 V was observed. **B–2** and **B–3** show similar redox potentials (Fig. 4b and 4c). For the dyads **FcB–1**, **FcB–2** and **FcB–3**, similar redox potentials attributed to the Bodipy moiety were observed, indicating a weak electronic interaction between the Fc and the Bodipy moieties in the dyads. The redox potentials of the Fc moiety overlaps with the free Fc added in the solution (except in the case of **FcB–3**). 1,2,3-triazole moiety give irreversible oxidation waves in the range of 0.3–0.6 V (vs. Ag/AgNO$_3$), this assignment was confirmed by **FcB–0** (see ESI †, Fig. S33).

In order to study the PET process of the dyads, the Gibbs free energy changes (ΔG°_{CS}) of the PET processes of the dyads was calculated according to the Weller equation (Eq. 2 and Eq. 3),[34] and charge separation energy states (E_{CS}) was calculated according to the Eq. 4.

$$\Delta G^{0}{}_{\mathrm{CS}} = e[E_{OX} - E_{RED}] - E_{00} + \Delta G_{\mathrm{S}} \qquad \text{(Eq. 2)}$$

$$\Delta G_{\mathrm{S}} = -\frac{e^2}{4\pi\varepsilon_{\mathrm{S}}\varepsilon_0 R_{\mathrm{CC}}} - \frac{e^2}{8\pi\varepsilon_0}\left(\frac{1}{R_D} + \frac{1}{R_{\mathrm{A}}}\right)\left(\frac{1}{\varepsilon_{REF}} - \frac{1}{\varepsilon_S}\right) \qquad \text{(Eq. 3)}$$

$$E_{CS} = e\left[E_{OX} - E_{RED}\right] + \Delta G_{\mathrm{S}} \qquad \text{(Eq. 4)}$$

where ΔG_S is the static Coulombic energy, which is described by Eq. 2. e = electronic charge, E_{OX}= half-wave potential for one-electron oxidation of the electron-donor unit, E_{RED} = half-wave potential for one-electron reduction of the electron-acceptor unit; note herein the anodic and cathodic peak potentials were used

Table 1 Photophysical Properties of **FcB–1**, **FcB–2**, **FcB–3**, **B–1**, **B–2** and **B–3** [a]

Comp.	$\lambda_{abs}{}^{b}$ /nm	ε [c]	$\lambda_{em}{}^{d}$	τ [e]/ ns	τ_T [f] (μs)	Φ_Δ	Φ [h]	$k_{ET}{}^{i}$ (s^{-1})
FcB–1	504	7.78	514	0.42 (85.2%), 4.29 (14.8%)	–[j]	–[j]	8.3%	(2.11 ± 0.11) × 10^9
FcB–2	538	8.02	551	0.18 (91.7%), 4.73 (8.3%)	–[j]	–[j]	4.9%	(1.39 ± 0.07) × 10^9
FcB–3	505	6.34	518	0.64 (19.0%), 2.78 (81.0%)	–[j]	–[j]	0.08%	(1.15 ± 0.06) × 10^9
B–1	504	9.18	514	3.72 (100%)	–[j]	–[j]	81%	–[j]
B–2	537	8.84	553	0.24(100%)	83.96	0.74[g]	7.8%	–[j]
B–3	506	7.05	518	2.42 (100%)	–[j]	–[j]	25.4%	–[j]

[a] The excitation wavelength for **B–1, B–3, FcB–1** and **FcB–3** were 480 nm, **B–2, FcB–2** were 515 nm (1.0 × 10^{-5} M, 20 °C In toluene). [b] Absorption wavelength. [c] Molar extinction coefficient, ε : 10^4 M^{-1} cm^{-1}. [d] Fluorescence emission wavelength. [e] Fluorescence lifetimes in Toluene. [f] Triplet state lifetimes. [g] Quantum yield of singlet oxygen ($^1O_2$), with 2,6-diiodo-Bodipy as standard (Φ_Δ = 0.79 in CH_2Cl_2), λ_{ex} = 526.5 nm. [h] Fluorescence quantum yields in Toluene, **B–1**, **B–3**, **FcB–1** and **FcB–3** with boron–dipyrromethene(Bodipy) (0.72 in THF) as the standard, **B–2** and **FcB–2** with 2,6–diiodo–Bodipy (0.027 in CH_3CN) as the standard. [i] The electron transfer rate constants in the dyads calculated with Eq 1. The error was estimated as ±5%. [j] Not applicable or not observed.

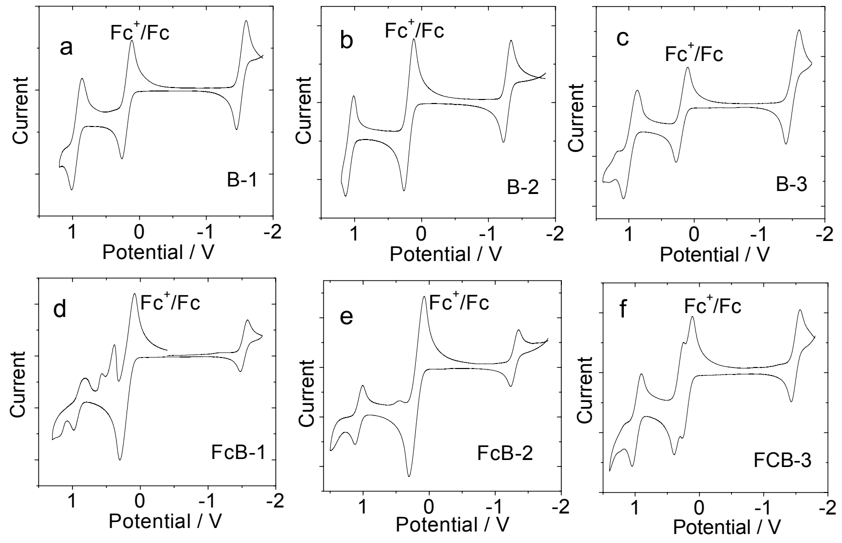

Fig. 4 Cyclic voltammogram of (a) **B–1**, (b) **B–2**, (c) **B–3**, (d) **FcB–1**, (e) **FcB–2**, (f) **FcB–3** (c = 5.0 × 10^{-4} M). for (a) – (e), c = 1.0 × 10^{-3} M. In deaerated CH_2Cl_2 solutions containing the compounds, 0.10 M Bu_4NPF_6 as supporting electrode, Ag/AgNO$_3$ as reference electrode, Scan rates: 100 mV/s. For all compounds Ferrocene (Fc) (c = 1.0 × 10^{-3} M) was used as internal reference. 20 °C.

Table 2 Electrochemical Data for Compound **B–1** , **B–2**, **B–3**, **FcB–1**, **FcB–2** and **FcB–3**

Compd	E_{ox} (V)	E_{red}(V)	ΔG_S(eV)			ΔG^0_{CS}(eV)			E_{CS} (eV)		
			Toluene	CH_2Cl_2	CH_3CN	Toluene	CH_2Cl_2	CH_3CN	Toluene	CH_2Cl_2	CH_3CN
B–1	+0.95	−1.53	$-^b$	$-^b$	$-^b$	$-^b$	$-^b$	$-^b$	$-^b$	$-^b$	$-^b$
B–2	+1.08	−1.28	$-^b$	$-^b$	$-^b$	$-^b$	$-^b$	$-^b$	$-^b$	$-^b$	$-^b$
B–3	+0.97	−1.50	$-^b$	$-^b$	$-^b$	$-^b$	$-^b$	$-^b$	$-^b$	$-^b$	$-^b$
FcB–1	+0.19/+0.90	−1.53	+0.29	−0.09	−0.20	-0.42^c	-0.82^c	-0.92^c	+2.02	$+1.63^c$	$+1.52^c$
FcB–2	+0.18/+1.10	−1.30	+0.29	−0.09	−0.20	-0.49^c	-0.89^c	-0.99^c	+1.78	$+1.38^c$	$+1.28^c$
						$+0.25^d$	-0.15^d	-0.25^d	$-^b$	$-^b$	$-^b$
FcB–3	+0.32/+0.97	−1.50	+0.49	−0.12	−0.29	-0.12^c	-0.73^c	-0.90^c	+2.31	$+1.69^c$	$+1.53^c$

[a] Recorded with $[Bu_4N][PF_6]$ as the electrolyte in CH_2Cl_2 (0.1 M) at room temperature with a scan rate of 100 mV/s. Potentials are expressed as the half-wave potentials ($E_{1/2}$) in volts vs $Ag/AgNO_3$.For all compound using ferrocene as an internal reference ($c = 1.0 \times 10^{-3}$ M). [b] Not determined. $E_{0,0}$ of complexes was approximated by the energy levels of the excited states of [c] ^{1}BDPY*. [d] ^{3}BDPY*. 20 °C.

because in some cases the oxidation is irreversible. Potential $E_{1/2}$ cannot be derived, therefore the $E_{0,0}$ energy level was estimated from crossing point of normalized absorption and emission spectra in CH_2Cl_2 (for the singlet excited state) (see ESI †, Fig. S34); ε_S = static dielectric constant of the solvent, R_{CC} = center-to-center separation distance between the electron donor (Fc unit) and electron acceptor (Bodipy unit), determined by DFT optimization of the geometry R_{CC} (**FcB–1**) = 16.6 Å, R_{CC}(**FcB–2**) = 16.6 Å and R_{CC}(**FcB–3**) = 12.8 Å. R_D is the radius of the ferrocene part based electron donor, R_A is the radius of the electron acceptor, ε_{REF} is the static dielectric constant of the solvent used for the electrochemical studies, ε_0 permittivity of free space($8.85\times10^{-12}m^{-3}kg^{-1}s^4A^2$). The solvents used in the calculation of free energy of the electron transfer are toluene (ε_S = 2.4), CH_2Cl_2 (ε_S = 9.1), CH_3CN (ε_S = 37.5). 20 °C.

Based on these parameters, for **FcB–2** in CH_2Cl_2, ΔG_S is calculated as −0.09 eV. For **FcB–2**, we assume that the singlet electron transfer from the electron donor to the electron acceptor is faster than any electron transfer, or charge separate. With the singlet excited state of the energy donor was populated (reference compound **B–2**), intersystem crossing (ISC) will occur. For compound **B–2**, ISC is a much faster than the fluorescence process, therefore we postulate that ISC will occur before any electron transfer process. $E_{0,0}$ of compound **B–2** was approximated by the T_1 state energy level (1.52 eV).[33] With reference **B–2** as electron acceptor, then the $\Delta G°_{CS}$ = 0.18−(−1.30) − 1.52 − 0.09 = −0.15 eV. Therefore the triplet excited state localized on the electron acceptor part (**B–2**) is likely to oxidize the energy donor Fc part.

If the electron transfer from the electron donor to the acceptor occurs at the singlet excited state of electron donor (reference unit **B–2**), then $E_{0,0}$ of compound **B–2** is approximated as 2.28 eV. With reference **B–2** as electron acceptor, the $\Delta G°_{CS}$ = 0.18−(−1.30) − 2.28− 0.09 = −0.89 eV. Based on these analyses, the intramolecular electron transfer in **FcB–2** is much significant from electron donor (ferrocene part) to electron acceptor (**B–2**) at the singlet excited state. Similarly the Gibbs free energy changes of **FcB–1** and **FcB–3** was also calculated and the data was summarized in Table 2. It was found that the PET is exothermic for the dyads, and the Gibbs free energy changes of the PET is more negative in polar solvents than that in less polar solvents.

Switching of the Fluorescence of the Dyads with Redox Methods

Previously the ferrocene/ferrocinium (Fc/Fc^+) pair transformation in Fc-PDI dyad was used for switching of the fluorescence of PDI moiety.[38] Herein the switching of the fluorescence of dyad **FcB–1** was achieved with an electrochemical method (Fig. 5. The fluorescence spectra were recorded with a spectraelectrochemical cuvette).

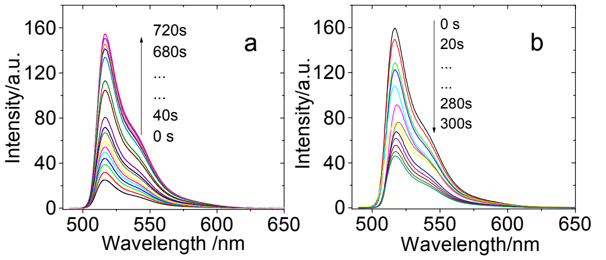

Fig. 5 (a) The fluorescence intensity changes of **FcB–1** (λ_{ex} = 480 nm), upon oxidation under 0.7 V versus $Ag/AgNO_3$ (from neutral state to oxidative state of Fc^+). (b) The fluorescence intensity changes of **FcB–1** (λ_{ex} = 480 nm), upon reduction under −0.3 V versus $Ag/AgNO_3$ (from oxidative state to neutral state of Fc). Potentials were applied with a electrochemical workstation. The sample solutions contained the compound **FcB–1** (5.0×10^{-4} M) and 0.1 M $[Bu_4N][PF_6]$ as the supporting electrolyte in CH_3CN, the fluorescence spectra were recorded upon 480 nm excitation. The spectra were recorded in situ with a spectroelectrochemical cuvette. 20 °C.

Upon oxidation of the Fc moiety (0.7 V was imposed, vs $Ag/AgNO_3$) to Fc^+, the fluorescence band at 517 nm was enhanced gradually, a maximum of 7.0−fold enhancement was observed (Fig. 5a). This fluorescence enhancement upon oxidation of Fc may be attributed to the cease of the PET with Fc as the electron donor because Fe^{3+} is unable to be oxidized further. Upon reduction, i.e. $Fc^+ \rightarrow Fc$ transformation (−0.3 V imposed on the working electrode, vs. $Ag/AgNO_3$), the fluorescence band at 517 nm was decreased (Fig. 5b). Similar results were observed for **FcB–3** (see ESI †, Fig. S35).

As the fluorescence of a PDI-Fc triad was modulated by the electrochemical approach of reversible oxidation/reduction of Fc moiety.[38,40] The electrochromism of Fc-Bodipy conjugate (the two chromophores were connected by π-conjugation linker) was studied, but the switching of the fluorescence of the dyad was not studied.[41] However, no switching of the fluorescence of Fc-Bodipy dyad via electrochemical reduction/oxidation has been reported.[24] The fluorescence intensity of **FcB–3** was increased by about 20–fold (see ESI †, Fig. S36).

The fluorescence intensity was recovered after each step and found to be rapidly and almost completely recovered on completion of the step; thus, the reversibility of the switching process was proved. As a result, a fast and vigorous redox–fluorescence switch can be established with dyads **FcB–1** and **FcB–3** (Fig. 6), by taking advantage of the properties of the ferrocene electron donor and the Bodipy as a fluorescent read-out unit.[42]

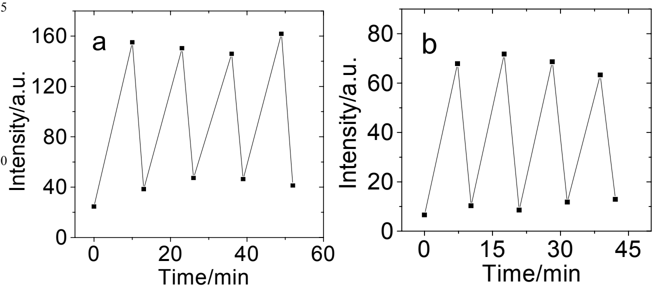

Fig. 6 Chronoamperometric analysis of (a) **FcB–1** ($c = 5.0\times10^{-4}$ M in CH_3CN), the potentials were switched at +0.7 V for 600 s (for oxidation) and then −0.3 V for 300 s (for reduction), the fluorescence intensity at 512 nm was monitored (λ_{ex} = 480 nm). (b) **FcB–3** ($c = 5.0 \times 10^{-4}$ M) the potentials were switched at +0.9 V for 440 s (for oxidation) and −0.2 V for 200 s (for reduction), the fluorescence intensity at 514 nm was monitored (λ_{ex} = 480 nm). 0.1 M $[Bu_4N][PF_6]$ as the supporting electrolyte, The potentials are versus $Ag/AgNO_3$. 20 °C.

To verify the reversibility of the electrochemically controlled fluorescence switching, different scanning rates were used to check the complete electrochemical reversibility of the Fe^{II}/Fe^{III} redox couple of the dyads (see ESI †, Fig. S36).[42] These results show the reversibility of the redox process is excellent. Thus our present study offers a new approach for controlling the fluorescence of Bodipy.

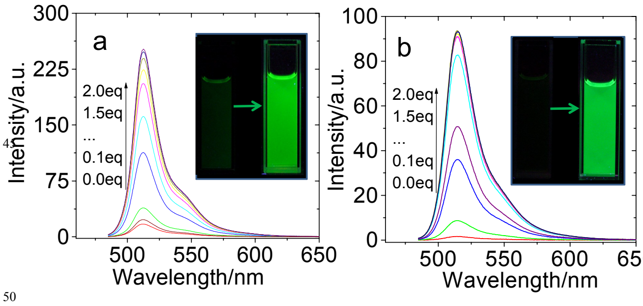

Fig. 7 Fluorescence spectra of (a) **FcB–1** ($c = 1.0 \times 10^{-5}$ M), (b) **FcB–3** ($c = 1.0 \times 10^{-5}$ M) in THF in the presence of different amounts of $Fe(ClO_4)_3$ (λ_{ex} = 480nm). The inset shows the photographs of the emission changes in the solution with $Fe(ClO_4)_3$ added, $c = 1.5 \times 10^{-5}$ M in THF, 20 °C.

Chemical oxidation experiments were also performed to confirm the fluorescence of Bodipy moiety can be switched-ON with oxidant. With increasing the concentration of $Fe(ClO_4)_3$ in the solution, the fluorescence emission of **FcB–1** was enhanced (Fig. 7a), a distinct fluorescence switching ON effect was observed (inset of Fig. 7a). Similar results were observed for **FcB–3** (Fig. 7b).

In order to determine the evolution of the fluorescence intensity after the addition of one equivalent of $Fe(ClO_4)_3$, the fluorescence emission was recorded every minute. The fluorescence intensity enhancement is saturated after about 20 min for **FcB–1** and 15 min for **FcB–3** (see ESI †, Fig. S37– S38), respectively. The effect of the oxidizing agent on the fluorescence intensity of **B-1** and **B-3** was not obvious (see ESI †, Fig. S39). More than 80% of the fluorescence intensity of Bodipy chromophores was recovered. This result is much higher than previously reported 33.2%.[40,42–44] However, no suitable reductant was found to switch OFF the fluorescence of Bodipy dyad, this situation is similar to a previous study on the switching of the fluorescence of Fc–PDI and Fc–porphyrin with $Fe(ClO_4)_3$.[40,44]

The switching of the fluorescence of Bodipy moiety in the dyads was summarized in Scheme 2 and Scheme S1. Upon photoexcitation of the Bodipy moiety, the singlet excited state in **FcB-1** was quenched by the PET process, thus the fluorescence was substantially reduced as compared with the emission of the Bodipy moiety. Upon oxidation of the Fc moiety in the dyad, the PET process is inhibited, as a result, the fluorescence of the Bodipy was recovered.

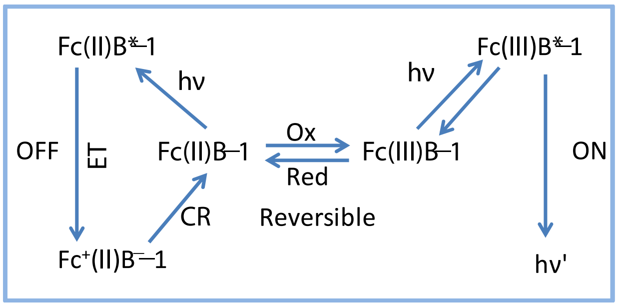

Scheme 2. Mechanism of Photoinduced Electron-Transfer Quenching and Off/On Redox Switching of Fluorescence Emission for Ferrocene–Bodipy dyad

The Effect of Fc on the Triplet Excited State of Bodipy

It is well known that long-lived triplet excited state are important for photocatalysis,[1–3] photodynamic therapy (PDT),[4–11] TTA upconversion[8,33] and molecular devices[4,5]. However, the quenching effect of Fc on the triplet excited state of Bodipy was rarely studied. Click 1,2,3-triazole as the linker was selected to construct **FcB–2**. From electron and energy transfer respectively, this kind of linker benefits to further study the quenching effect of Fc on the triplet excited state of organic chromophores (e.g. 2,6-diiodoBodipy). Triplet-triplet annihilation (TTA) upconversion, an important application of triplet photosensitizer,[4,10,30,33] provide an indirect way to study the quenching effect of Fc on the triplet excited state. Herein, TTA upconversion with **FcB–2** as the triplet photosensitizer and perylene as the triplet acceptor was studied, and no TTA upconversion luminescence was observed (see ESI †, Fig. S40).

In order to study the reason of the lack of TTA upconversion with **FcB–2** as the triplet photosensitizer, we carried out two control experiments. **B–2** was used as the triplet photosensitizer and perylene as the triplet acceptor/emitter, strong TTA

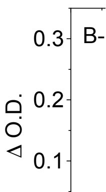

upconversion was observed (Fig. 8a). With addition of ferrocene into the mixture, however, the TTA upconversion intensity was reduced. Two facts may be responsible for this quenching effect, i.e. quenching of the fluorescence of perylene by Fc, or quenching of the triplet excited states (either the triplet excited state of **B–2** or the triplet state of perylene). Thus we studied the fluorescence variation of perylene in the presence of Fc (Fig. 8b). The results show that the fluorescence of perylene was hardly quenched by Fc. Therefore, we propose that the Fc is a quencher for the triplet excited state.

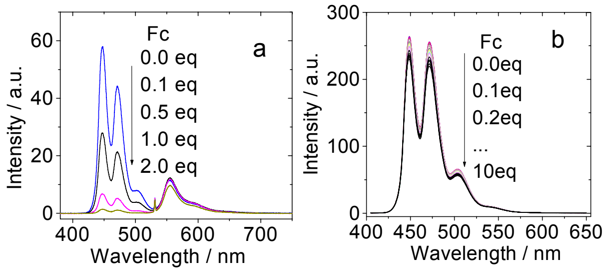

Fig. 8 (a) The upconverted perylene fluorescence and the residual fluorescence of **B–2** with increasing ferrocene concentration (λ_{ex} = 532 nm). c[**B–2**] = 1.0 × 10^{-5} M, c[perylene] = 4.0 × 10^{-5} M in deaerated Toluene. (b) The fluorescence emission of perylene with increasing amount of ferrocene added. c [perylene] = 4.0 × 10^{-5} M in deaerated toluene, 20 °C.

Triplet excited state of **FcB–2** and the reference **B–2** in toluene were studied with the nanosecond transient absorption spectroscopy (Fig. 9). Normal nanosecond transient absorption spectra were observed for **B–2**, which is in accordance with previous report (Fig. 9a and inset).[30] For **FcB–2** in toluene, no transient signal was detected with our nanosecond transient absorption spectrometer (time-resolution of 10 ns) (Fig. 9b and inset). Similar result was observed for **FcB–2** in acetonitrile (see ESI †, Fig. S41).

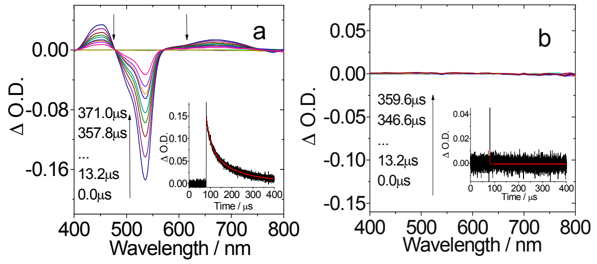

Fig. 9 Comparison of the nanosecond transient absorption spectroscopy of (a) **B–2** and (b) **FcB–2** (c) Decay trace of the transient of **B–2** and **FcB–2** at 525 nm. Excited with 532 nm nanosecond pulsed laser. c = 1.0 × 10^{-5} M in deaerated toluene, 20 °C.

It should be pointed out that toluene is an non polar solvent, and intramolecular electron transfer of **FcB–2** is hardly occurs ($\Delta G^0_{CS} > 0$ eV) in toluene. Therefore, we propose that, in toluene (apolar solvent), triplet-triplet energy transfer (TTET) from the Bodipy moiety to Fc may be responsible for the quenching of the triplet excited state of the Bodipy moiety.[45] However, the triplet state of Fc shows a very weak excited state absorption (ESA) at 617 nm (ε = 450 M^{-1} cm^{-1}).[26] There is no significant transient signal in nanosecond transient absorption spectra assigned to the T_1 state of Fc,[46] which increases the difficulty to the study.

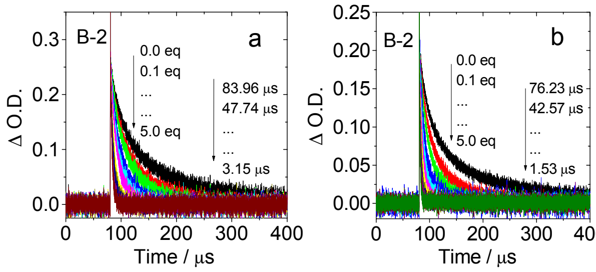

Fig. 10 Quenching of the triplet state lifetime of **B–2** with increasing the concentration of ferrocene, (a) **B–2**, c [ferrocene] = 0 –5.0 × 10^{-5} M. In deaerated toluene. (b) **B–2**, c [ferrocene] = 0 – 5.0 × 10^{-5} M. In deaerated CH_3CN. 25 °C.

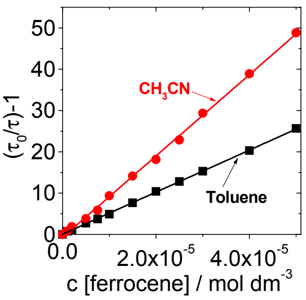

Fig. 11 Stern–Volmer plots for triplet state lifetime quenching of **B–2** with increasing the concentration of ferrocene, upon pulsed excitation (λ_{ex} = 515 nm). c [**B–2**] = 1.0 × 10^{-5} M in deaerated toluene and CH_3CN, 20 °C.

Fortunately, the T_1 state energy level of Fc could be calculated by Stern-Volmer quenching constant (Fig. 10 and Fig. 11) and Eq. 5. [25,27,47] The triplet state lifetime of **B–2** was reduced gradually with increasing the concentration of Fc (Fig. 11, Table S1). The Stern-Volmer quenching curve was plotted (Fig. 11). Given that T_1 state of Bodipy was quenched by Fc through the TTET process, the energy transfer rate constants should be given by Eq. 5.[25,47]

$$k_q = k_D \cdot \frac{1}{1+\exp(-\Delta E_T/kT)} \qquad \text{(Eq. 5)}$$

Where k_D is the diffusion-controlled rate constants, k is Boltzmann's constant and $\Delta E_T = E_T(\text{Donor}) - E_T(\text{Acceptor})$.

The Stern–Volmer quenching constant of **B–2**/Fc was calculated as K_{SV} = (5.09 ± 0.14) × 10^5 M^{-1} in toluene. The bimolecular quenching constant k_q was calculated as (6.06 ± 0.17) × 10^9 M^{-1} s^{-1} in toluene (Table S2) according to Eq. 6. τ_0 is the triplet state lifetime of the triplet energy donor.

$$k_q = K_{SV}/\tau_0 \qquad \text{(Eq. 6)}$$

The diffusion–controlled bimolecular quenching rating constants k_D, can be calculated with the Smoluchowski equation (Eq. 7).

$$k_D = 4\pi RND/1000 = \frac{4\pi N}{1000}\left(R_{\mathrm{f}} + R_{\mathrm{q}}\right)\left(D_{\mathrm{f}} + D_{\mathrm{q}}\right) \qquad \text{(Eq. 7)}$$

D is the sum of the diffusion coefficients of the energy donor (D_{f}) and quencher (D_{q}), N is Avogadro's number. R is the collision radius, the sum of the molecule radii of the energy donor (R_{f}) and the quencher (R_{q}).

Diffusion coefficients can be obtained from Stokes–Einstein equation (Eq. 8).

$$D = kT/6\pi\eta R \qquad \text{(Eq. 8)}$$

k is Boltzmann's constant, η is the solvent viscosity, R is the molecule radius. For the molecule radii of the energy donor (**B–2**) is 4.34Å and that of quencher (Fc) is 1.75 Å. According to equation 7 the diffusion coefficients of the energy donor (**B–2**) is 8.43×10^{-6} cm^2 s^{-1} and that of quencher (Fc) is 2.09×10^{-5} cm^2 s^{-1} (in toluene at 20 °C). Thus k_{D} was calculated as 1.35×10^{10} M^{-1} s^{-1}.

The triplet energy transfer rate constant was calculated as $(6.06 \pm 0.17) \times 10^9$ M^{-1} s^{-1} (Table S2). Assuming that **B–2** triplet excited state is quenched by energy transfer from **B–2** triplet excited state to that of Fc, the triplet level of Fc can be calculated by Eq. 5. From the values $k_{\mathrm{D}} = 1.35 \times 10^{10}$ M^{-1} s^{-1} and $k_{\mathrm{q}} = (6.06 \pm 0.17) \times 10^9$ M^{-1} s^{-1} in toluene, $\Delta E_T = E_T$(**B–2**) $-E_T$(Fc) = -5.17×10^{-3} eV. Thus, the triplet state level of Fc is estimated to be 1.53 eV.[25,27] The triplet state level of Fc is close to **B–2** and previous report.[25,27] Thus TTET mechanism is responsible for the quenching of the triplet excited state of **B–2** in toluene.

Interestingly, the quenching effect is more significant in polar solvent such as acetonitrile than that in toluene (Fig. 10 and Fig. 11). It may be due to the lower energy level of charge-separated state in polar solvent. In CH_3CN, the energy of charge separated state is calculated as 1.28 eV ($E_{\mathrm{CS}} = + 0.18 - (-1.30) - 0.20 = +1.28$ eV). The energy level of charge separate state is much lower than that of triplet excited state of **B-2** and even Fc, indicating that intermolecular electron transfer may be responsible for the faster quenching effect of **FcB-2** in CH_3CN. Thus both the PET and TTET are responsible for the quenching of the triplet excited state of **B–2**.

Conclusions

In summary, three different Bodipy-ferrocene (Fc) dyads with different linker between the Bodipy and the Fc moieties were prepared. Reversible electrochemical switching of the fluorescence of Bodipy fluorophore was realized with Bodipy-ferrocene (Fc) dyads. The quenching of the triplet excited state of Bodipy by Fc was also investigated. The photophysical properties of the dyads were studied with stead-state UV–vis absorption spectroscopy, luminescence, electrochemical characterization, time-resolved fluorescence and nanosecond transient absorption spectroscopies. Two quenching mechanisms, PET and triplet-triplet-energy transfer, are responsible for the intramolecular and intermolecular quenching of the triplet excited state of the photosensitizer.

Acknowledgement

We thank the NSFC (20972024, 21273028, 21302224, 21421005 21473020 and 51372277), the Royal Society (UK) and NSFC (China-UK Cost-Share Science Networks, 21011130154), Ministry of Education (SRFDP-20120041130005) Program for Changjiang Scholars and Innovative Research Team in University [IRT_13R06], the Fundamental Research Funds for the Central Universities (DUT14ZD226) and Dalian University of Technology (DUT2013TB07), China Postdoctoral Science Foundation (2014M560590), Shandong Provincial Natural Science Foundation (ZR2013BQ028), Project of Science and Technology Program for Basic Research of Qingdao (14-2-4-47-jch) and the State Key Laboratory of Fine Chemicals (KF1203) for financial support.

Notes

[a] *State Key Laboratory of Fine Chemicals, School of Chemical Engineering, Dalian University of Technology, E-208 West Campus, 2 Ling Gong Rd., Dalian 116024, P. R. China.*
E-mail: zhaojzh@dlut.edu.cn Web: http://finechem2.dlut.edu.cn/photochem;

[b] *State Key Laboratory of Heavy Oil Processing, China University of Petroleum, Qingdao 266580, P. R. China. Fax: +86 532 8698 1787, Tel.: +86 532 8698 3452. E-mail: wumb@upc.edu.cn*

[¶] *These authors contributed equally to this work.*

†*Electronic Supplementary Information (ESI) available: Molecular structure characterization data, absorption and fluorescence emission data. See DOI: 10.1039/b000000x/*

References

1 D. P. Hari and B. Koenig, *Angew. Chem. Int. Ed.,* 2013, **52**, 4734–4743.
2 L. Shi and W. Xia, *Chem. Soc. Rev.,* 2012, **41**, 7687–7697.
3 Y. Xi, H.Yi and A. Lei, *Org. Biomol. Chem.,* 2013, **11**, 2387–2403.
4 S. Erbas-Cakmak and E. U. Akkaya, *Angew. Chem. Int. Ed.,* 2013, **52**, 11364–11368.
5 O. AltanáBozdemir, *Chem. Sci.,* 2013, **4**, 858–862.
6 (*a*) B. De Salvo, J. Buckley and D. Vuillaume, *Curr. Appl. Phys*., 2011, **11**, 49–57; (*b*) T. Tsujioka and H.Kondo, *Appl Phys Lett.*, 2003, **83**, 937–939.
7 (*a*) A. R. Lippert, G. C. Van de Bittner, C. J. Chang, *Acc. Chem. Res.*, 2011, **44**, 793–804; (*b*) E. L. Que, D. W. Domaille and C. J. Chang, *Chem. Rev.,* 2008, **108**, 1517– 1549.
8 J. Zhao, W. Wu, J. Sun and S. Guo, *Chem. Soc. Rev.*, 2013, **42**, 5323–5351.
9 Y. You and W. Nam, *Chem. Soc. Rev.,* 2012, **41**, 7061–7084.
10 P. Batat, M. Cantuel, G. Jonusauskas, L. Scarpantonio, A. Palma, D. F. O'Shea and N. D. McClenaghan, *J. Phys. Chem. A.,* 2011, **115**, 14034–14039.
11 D. O. Frimannsson, M. Grossi, J. Murtagh, F. Paradisi and D. F. O'Shea, *J. Med. Chem.,* 2010, **53**, 7337–7343.
12 S. O. McDonnell, M. J. Hall, L. T. Allen, A. Byrne, W. M. Gallagher and D. F. O'Shea, *J. Am. Chem. Soc.,* 2005, **127**, 16360–16361.
13 S. G. Awuah and Y. You, *RSC Adv.,* 2012, **2**, 11169–11183.
14 Z. Guo, W. Zhu, H. Tian, *Chem. Commun.,* 2012, **48**, 6073–6084.
15 X. Chen, Y. Zhou, X. Peng and J. Yoon, *Chem. Soc. Rev.,* 2010, **39**, 2120–2135.
16 Y. Chen, L. Wan, X. Yu, W. Li, Y. Bian and J. Jiang, *Org. Lett.,* 2011, **13**, 5774–5777.
17 L. Niu, Y. Guan, Y. Chen, L. Wu, C. Tung and Q. Yang, *J. Am. Chem. Soc.,* 2012, **134**, 18928–18931.
18 A. M. Bugaj, *Photochem. Photobiol. Sci.* 2011, **10**, 1097–1109.
19 P. Majumdar, R. Nomula, J. Zhao, *J. Mater. Chem. C*, 2014, **2**, 5982–5997.
20 J. Tian, L. Ding, H. Xu, Z. Shen, H. Ju, L. Jia, L. Bao and J.Yu, *J. Am. Chem. Soc.,* 2013, **135**, 18850–18858.
21 S. Fery-Forgues and B. Delavaux-Nicot, *J. Photochem. Photobiol.: A,* 2000, **132**, 137–159.

22 T. Nakamura, H. Kanato, Y. Araki, O. Ito, K. Takimiya, T. Otsubo and Y. Aso, *J. Phys. Chem. A,* 2006, **110**, 3471−3479.

23 C. A. Wijesinghe, M. E. El-Khouly, J. D. Blakemore, M. E. Zandler, S. Fukuzumi and F. D'Souza, *Chem. Commun.* 2010, **46**, 3301−3303.

24 X. Yin, Y. Li, Y. Zhu, X. Jing, Y. Li, D. Zhu, *Dalton Trans.,* 2010, **39**, 9929−9935.

25 M. Kikuchi, K. Kikuchi, H. Kokubun, *Bull. Chem. Soc. Jpn.,* 1974, **47**, 1331−1333.

26 M. Supur, M. E. El-Khouly, J. H. Seok, J. H. Kim, K.Y. Kay and S. Fukuzumi, *J. Phys. Chem. C,* 2010, **114**, 10969−10977.

27 F. D'Souza, M. E. Zandler, P. M. Smith, G. R. Deviprasad, K. Arkady, M. Fujitsuka and O. Ito, *J. Phys. Chem. A,*. 2002, **106**, 649−656.

28 M. Supur, M. E. El-Khouly, J. H. Seok,; K.Y. Kay and S.Fukuzumi, *J. Phys. Chem. A,* 2011, **115**, 14430−14437.

29 A. N. Amin, M. E. El-Khouly, N. K. Subbaiyan, M. E. Zandler, M. Supur, S. Fukuzumi and F. D'Souza, *J. Phys. Chem. A,* 2011, **115**, 9810−9819.

30 A. Loudet and K. Burgess, *Chem. Rev.,* 2007, **107**, 4891−4932.

31 G. Ulrich, R. Ziessel and A. Harriman, *Angew. Chem. Int. Ed.,* 2008, **47**, 1184−1201.

32 H. Lu, J. Mack, Y. Yang and Z. Shen, *Chem. Soc. Rev.,* 2014, **43**, 4778−4823.

33 W. Wu, H. Guo, W. Wu, S. Ji and J. Zhao, *J. Org. Chem.,* 2011, **76**, 7056−7064.

34 M. E. El-Khouly, A. N. Amin, M. E. Zandler, S. Fukuzumi and F. D'Souza, *Chem. Eur. J.,* 2012, **18**, 5239−5247.

35 Z. Kostereli, T. Ozdemir, O. Buyukcakir and E. U. Akkaya, *Org. Lett.,* 2012, **14**, 3636−3639.

36 T. Bura, F. Nastasi, F. Puntoriero, S. Campagna and R. Ziessel, *Chem. Eur. J.,* 2013, **19**, 8900−8912.

37 R. Zhang, Y. Wu, Z. Wang, W. Xue, H. Fu and J. Yao, *J. Phys. Chem. C,* 2009, **113**, 2594−2602.

38 N. J. Turro, V. Ramamurthy and J. C. Scaiano, University science books: 2009.

39 R. Zhang, Z. Wang, Y. Wu, H. Fu and Yao, J. *Org. Lett.,* 2008, **10**, 3065−3068.

40 J. J. Apperloo, C. Martineau, P. A. van Hal, J. Roncali and R. *J.* Janssen, *Phys. Chem. A,* 2002, **106**, 21−31.

41 X. Yin, Y. Li, Y. Li, Y. Zhu, X. Tang, H. Zheng and Zhu, D. *Tetrahedron,* 2009, **65**, 8373−8377.

42 R. Martínez, I. Ratera, A. Tárraga, P. Molina and J. Veciana, *Chem. Commun.,* 2006, 3809−3811.

43 S. Leroy-Lhez, J. Baffreau, L. Perrin, E. Levillain, M. Allain, M. Blesa and P. Hudhomme, *J. Org. Chem.,* 2005, *70*, 6313-6320.

44 Zhou, Y.; Ngo, K. T.; Zhang, B.; Feng, Y.; Rochford, J. *Organometallics*, 2014, **33**, 7078–7090.

45 Y. Araki, Y. Yasumura and O. Ito, *J. Phys. Chem. B,*. 2005, **109**, 9843−9848.

46 A. D. Quartarolo, N. Russo and E. Sicilia, *Chem. Eur. J.,* 2006, **12**, 6797−6803.

47 W. E. Ford and P. V. Kamat, *J. Phys. Chem.,* 1987, **91**, 6373−6380.

Graphical Contents Entry:

Preparation of Bodipy-Ferrocene Dyads and Modulation of the Singlet/Triplet Excited State of Bodipy via Electron Transfer and Triplet Energy Transfer

Xueyan Wu, ¶ [a,b]Wenting Wu,¶[b] Xiaoneng Cui,[a] Jianzhang Zhao[a]* and Mingbo Wu[b],*

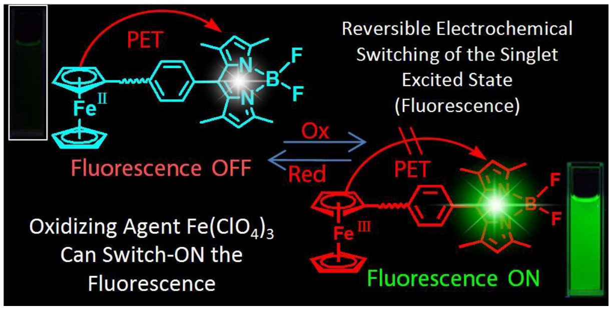

Bodipy-ferrocene dyads were prepared for reversible electrochemical switching of the singlet excited state (fluorescence), as well as the triplet excited states of Bodipy.